Article **Journal-Mathematical and Quantitative Methods**
June, 2022 Vol.6 No.10 8-17

Unbalance identification method based on SINDy applied to an SFD rotordynamic system

Método de identificación de desbalance basado en SINDy aplicado a un sistema rotodinámico soportado por un SFD

ZIRION-FLORES, Maximiliano†, ESCOBEDO-ALVA, Jonathan Omega, TORRES-CEDILLO, Sergio Guillermo* and REYES-SOLIS, Alberto

SEPI-ESIME TIC. IPN, Av. Ticomán 600, San José Ticomán, C.P. 07340, Ciudad de México, México
Centro Tecnológico Aragón, FES- UNAM, Av. Rancho Seco s/n, C.P. 57130, Edo. de México, México Edo. de México

ID 1st Author: *Maximiliano, Zirion-Flores* / **ORC ID**: 0000-0002-0621-6182, **CVU CONACYT ID**: 1109407

ID 1st Co-author: *Jonathan Omega, Escobedo-Alva* / **ORC ID**: 0000-0001-8429-0591, **CVU CONACYT ID**: 230868

ID 2nd Co-author: *Sergio Guillermo, Torres-Cedillo* / **ORC ID**: 0000-0002-3297-6409, **CVU CONACYT ID**: 229481

ID 3rd Co-author: *Alberto, Reyes-Solís* / **ORC ID**: 0000-0002-5208-8919

DOI: 10.35429/JMQM.2022.10.6.8.17 Received March 28, 2022; Accepted June 10, 2022

Abstract

In recent years, there has been an increasing interest in Data Science and Machine Learning in different topics like financial and health, this have led to start using these methods on engineer applications. This paper is focus on identify the equivalent unbalance on Squeeze Film Damper – SFD bearing using a recent machine learning technique "Sparse Identification of Nonlinear Dynamics – SINDy". Four different cases will be examined from Bonello's work, all of which we introduce 4 different conditions of noise to the acceleration of the system. The data for this work was obtained via a simulation of the SFD system reported on Bonello's thesis. From the simulation only the last 20 cycles were used to feed the SINDy. This study uses a combinatorial polynomial search space over preselected functions with the purpose to identify the equivalent imbalances. Both hyperparameters: the degree of the combinatory k and the threshold value λ remaining static during all the study. There was no error between the original equations and the identified system.

Sparse Identification of Nonlinear dynamics, Squeeze Film Damper, Equivalent unbalance

Resumen

Mediante el algoritmo de aprendizaje automático de "Identificación escasa de dinámicas no lineales – Sparse identification of nonlinear dynamics SINDy" se identificó el desbalance equivalente en un sistema rotodinámico soportado por un cojinete del tipo squeeze film damper bearing – SFD. Se identificaron los desbalances equivalentes a 4 condiciones operativas estacionarias, teniendo como parámetro de entrada la aceleración del sistema. Los datos empleados para la alimentación del algoritmo SINDy fueron obtenidos a través de una simulación del sistema rotodinámico SFD en Matlab usando un modelo matemático. Solamente fueron tomados los últimos 20 ciclos de la simulación. Un espacio de búsqueda de combinatoria polinomial de grado $K = 3$ fue empleado sobre las variables independientes del sistema para la identificación de los desbalances equivalentes empleando SINDy. De igual manera los desbalances equivalentes fueron obtenidos a tres distintas condiciones de ruido, esto con la finalidad de probar la robustez de SINDy. Los hiperparámetros de la herramienta; el grado de la combinatoria K y el valor de corte λ permanecieron estáticos durante los 4 casos bajo las distintas condiciones de ruido. El error entre el sistema modelado con las ecuaciones originales y el sistema identificado en este trabajo fue prácticamente nulo.

Identificación escasa de dinámicas no lineales, Desbalance equivalente, Rotodinámica

Citation: ZIRION-FLORES, Maximiliano, ESCOBEDO-ALVA, Jonathan Omega, TORRES-CEDILLO, Sergio Guillermo and REYES-SOLIS, Alberto. Unbalance identification method based on SINDy applied to an SFD rotordynamic system. Journal-Mathematical and Quantitative Methods. 2022. 6-10: 8-17

* Correspondence to Author (email: storresc@ipn.mx)
† Researcher contributing first author

1. Introduction

Currently, the wide digital expansion has had several consequences such as industry 4.0, the internet of things, and the personal use of the internet by 62.5% of the world's population, have led to a trend of collecting a large amount of data. To be exploited, several methodologies have been developed under the term "machine learning", with the purpose of predicting, clustering, discovering patterns of behaviors, classifying and making decisions. These methodologies are widely used in the areas of business, cellular applications and security, with beneficial results. These methodologies should be leveraged in the field of science and engineering (S. Brunton et al. 2020).

Unlike business areas where the goal of using these methodologies is prediction, science and engineering has specific needs such as:

- Interpretable models for scientific understanding and safety
- Models for general problems
- Models robust to noise
- Models obtained with little data or with low frequency of measurement.

In some or most cases, popular methods such as neural networks or regression models fail to satisfy one or more of the requirements of science and engineering.

The *Sparse Identification of Nonlinear Dynamics* (SINDy) algorithm presents an opportunity to take advantage of the benefits of machine learning methods in science and engineering by meeting their needs. This is because SINDy presents the advantage of identifying mathematical models using data (S. Brunton 2016).

Within the field of aeronautical engineering, a recurring problem is the unbalance of aerojet engines. A case identified in previous works are engines using "*squeeze film damper*" SFD type supports as are the Rolls-Royce engines of the BR700 family (V. Dicken et al. 2007), which are found in the following aircraft.

- Boeing 717, B-52
- Dassault Falcon 10X
- Gulfstream V, G550, G650, G700, G800
- Tupolev TU-334
- BAE Nimrod MRA4
- Bombardier Global Express

This unbalance generates maintenance costs because it is necessary to completely disassemble the engine to find the disc/blade that is out of balance. To solve this problem, inverse problem type approaches have been proposed using autonomous learning methods, mainly using neural networks, where the objective is to find the unbalance of the system using only the vibration of the engine casing (S. Torres et al. 2019).

An approach employing SINDy is presented in this paper, with the objective to prove the goodness of this type of methodologies. The work focuses on identifying the equivalent unbalance coefficient, using only the information of the acceleration, forces and periodic behaviors of the SFD system. These data were obtained through a simulation based on the work of Bonello (2002). Beyond the objective of this article, its purpose is to develop this type of methodologies so that in the future they can be used in more complex systems, such as solving inverse problems. This would lead to experimental applications with non-invasive techniques as in the research of S. Torres et al. (2019).

2. SFD Model

Squeeze-film Damper (SFD) bearings provide a very cost effective means of introducing damping into aero engine rotors. This is achieved by pumping oil into the annular gap between the outside of the bearing element and the SFD housing (see Figure 1).

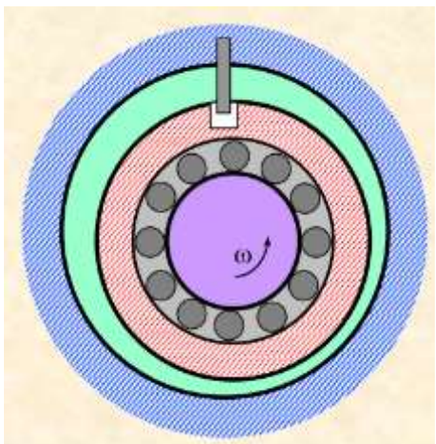

Figure 1 SFD Schematic
(San Andres 2018)

ISSN 2531-2979

In Figure 2, a rotodynamic system supported by a SFD that was modeled through the unsealed short bearing theory is illustrated. This system was employed by (P. Bonello, 2002) to validate the cavitation model "absolute zero cavitation model". This configuration consists of a rigid rotor supported on the right side by a self-aligning bearing and an unsupported SFD on the left side.

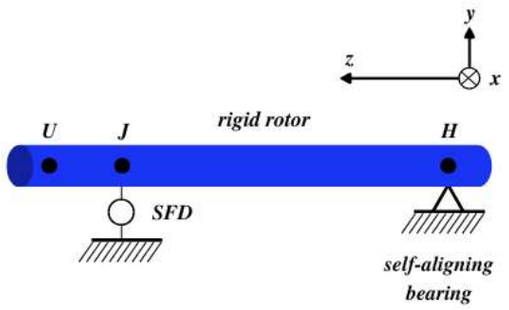

Figure 2 Rotodynamic system supported by a SFD *(R. Holmes et al. 1982)*

The system presented in Figure 2 is modeled in the work by Bonello (2002) using the following equations of motion

$$M_{R,J}\ddot{X}_J = Q_x + U_{eq,J}\Omega^2 \sin \Omega t$$

$$M_{R,J}\ddot{Y}_J = Q_y - U_{eq,J}\Omega^2 \cos \Omega t - W \quad (1)$$

where X_J and Y_J are the displacements in [m] of the rotor center J (Journal) from a fixed center of the pedestal, Ω is the rotational speed in [rad/s], $M_{R,J}$ is the effective mass in J, W is the static load in J and $U_{eq,J}$ is the equivalent unbalance in J. In the present work, the equations of motion (1) will be used to generate the data set required by the SINDy method and validate this technique to identify the unbalance $U_{eq,J}$ using different noise scenarios.

3. SINDy

SINDy is a machine learning tool where its main advantage is that it generates as output parameter mathematical models. To achieve this SINDy needs two data sets; the set of independent variables X and the set of dependent variables X resulting in the identification of a model such that $\dot{X}(X)$ (Brunton et al. 2016). For this, SINDy generates a search space Θ. The search space Θ will contain a set of possible functions created from X such that Θ(X), these search space functions are the candidates to describe $\dot{X}$ The goal of SINDy will be to solve the system.

$$\dot{\mathbf{X}} = \boldsymbol{\Theta}(\mathbf{X})\boldsymbol{\Xi} \quad (2)$$

Where the output of the algorithm, i.e. the identified model is in the sparse matrix Ξ in its coefficients and structure. The SINDy components have the following structure.

$$\mathbf{X} = \begin{bmatrix} x_1(t_1) & x_2(t_1) & \dots & x_M(t_1) \\ x_1(t_2) & x_2(t_2) & \dots & x_M(t_2) \\ \vdots & \vdots & \ddots & \vdots \\ x_1(t_N) & x_2(t_N) & \dots & x_M(t_N) \end{bmatrix}_{N\times M}$$

$$\dot{\mathbf{X}} = \begin{bmatrix} \dot{x}_1(t_1) & \dot{x}_2(t_1) & \dots & \dot{x}_L(t_1) \\ \dot{x}_1(t_2) & \dot{x}_2(t_2) & \dots & \dot{x}_L(t_2) \\ \vdots & \vdots & \ddots & \vdots \\ \dot{x}_1(t_N) & \dot{x}_2(t_N) & \dots & \dot{x}_L(t_N) \end{bmatrix}_{N\times L} \quad (3)$$

Each column of Θ(X) is a function.

$$\boldsymbol{\Theta}(\mathbf{X}) = \begin{bmatrix} f_1(x(t_1)) & f_2(x(t_1)) & \dots & f_S(x(t_1)) \\ f_1(x_i(t_2)) & f_2(x(t_2)) & \dots & f_S(x(t_2)) \\ \vdots & \vdots & \dots & \vdots \\ f_1(x(t_N)) & f_2(x(t_N)) & \dots & f_S(x(t_N)) \end{bmatrix}_{NXS} \quad (4)$$

The dimensions of the system are as follows.

$$\dot{\mathbf{X}}_{N\times L} = \boldsymbol{\Theta}(\mathrm{X})_{N\times S}\Xi_{S\times L} \quad (5)$$

N-Number of data
M-Number of independent variables
S- Number of proposed functions
L- Number of functions to identify or number of dependent variables.

3.1. Polynomial Combinatorial Search Space

A polynomial combinatorial combinatorial search space will be used for this work, having independent variables $X = [x_1, x_2, \cdots x_M]$. A search space can be created from the combination repeated k times, the size of the search space is described by the combination with repetition of $C'_{k(M)}$. For the search space to go through the whole set of possible polynomials, generated from X_M reaching up to degree k, it is necessary to add unity to our set of independent variables; so that$X_{M+1} = 1, x_1, x_2, \cdots x_M$, the size of the search space will be the combinatorial with repetition of degree k.

$$\mathbf{C}'_{k(M+1)} = [1_{N\times 1}\ C^1_{N\times M}\ C^k_{N\times R_k} \cdots C^K_{N\times R_K}\ ],$$
$$k = 2,3, \dots, K. \quad (6)$$

Where $R_k = (k+1)(M-1)$

The number of proposed functions is fined as follows

$$S = 1 + M + R_2 + R_3 + \cdots + R_k$$

As an example, the second and third elements of (6) would be as follows:

$$\mathbf{C}^1 = \begin{bmatrix} x_1(t_1) & x_2(t_1) & \cdots & x_M(t_1) \\ x_1(t_2) & x_2(t_2) & \cdots & x_M(t_2) \\ \vdots & \vdots & \vdots & \vdots \\ x_1(t_N) & x_2(t_N) & \cdots & x_M(t_N) \end{bmatrix}$$

$$\mathbf{C}^2 = \begin{bmatrix} x_1^2(t_1) & \cdots & x_1(t_1)x_2(t_1) & \cdots & x_M^2(t_1) \\ x_1^2(t_2) & \cdots & x_1(t_2)x_2(t_2) & \cdots & x_M^2(t_2) \\ \vdots & \vdots & \vdots & \vdots & \vdots \\ x_1^2(t_N) & \cdots & x_1(t_N)x_2(t_N) & \cdots & x_M^2(t_N) \end{bmatrix} \quad (7)$$

$\mathbf{C}^n$ It will then be a matrix with all the combinations between the different state variables that form monomials of degree *n*.

Finally, to clarify this structure, the following example is presented where *k*=3 and *M*=2.

$\mathbf{X}_M = [x\ , y]$,

$\mathbf{X}_{M+1} = [1, x, y]$,

$$\mathbf{X}_{M+1} = \begin{bmatrix} 1 & x(t_1) & y(t_1) \\ 1 & x(t_2) & y(t_2) \\ \vdots & \vdots & \vdots \\ 1 & x(t_N) & y(t_N) \end{bmatrix}_{N\times(M+1)},$$

$\mathbf{C}'_{k(M+1)} = [1_{N\times 1}\ C^1_{N\times M}\ C^2_{N\times R_2}\ C^3_{N\times R_3}\ ]$,

$R_2 = 3\ , R_3 = 4$,

Accordingly, you will have:

$S = 10$,

$$\mathbf{C}^1 = \begin{bmatrix} x(t_1) & y(t_1) \\ x(t_2) & y(t_2) \\ \vdots & \vdots \\ x(t_N) & y(t_N) \end{bmatrix},$$

$$\mathbf{C}^2 = \begin{bmatrix} x^2(t_1) & x(t_1)y(t_1) & y^2(t_1) \\ x^2(t_2) & x(t_2)y(t_2) & y^2(t_2) \\ \vdots & \vdots & \vdots \\ x^2(t_N) & x(t_N)y(t_N) & y^2(t_N) \end{bmatrix},$$

$$C^3 = \begin{bmatrix} x^3(t_1) & x^2(t_1)y(t_1) & x(t_1)y^2(t_1) & y^3(t_1) \\ x^3(t_2) & x^2(t_2)y(t_2) & x(t_2)y^2(t_2) & y^3(t_2) \\ \vdots & \vdots & \vdots & \vdots \\ x^3(t_N) & x^2(t_N)y(t_N) & x(t_N)y^2(t_N) & y^3(t_N) \end{bmatrix} \quad (8)$$

3.2. System resolution

The matrix $\Theta(X)_{N\times S}$ has a rectangular structure such that in most cases $N \gg S$, in addition Ξ, containing coefficients that rule out proposed functions, will be a sparse matrix, for such reasons it is necessary to use methods that solve systems with this type of matrices. For this work we will use least squares minimizing the Euclidean space under the norm-2.

$$\|b - ax\| \quad (9)$$

Together with an iterative cutoff function, which under a parameter λ cuts off all values below it (Brunton et el. 2016).

4. Lorenz attractor

To test the capabilities of SINDy and to clarify a little more its operation we will use a deterministic, chaotic, nonlinear and coupled system, as is the Lorenz Attractor, for this we will use a simulation of its mathematical model.

$$\begin{aligned} \dot{x} &= \sigma(y - x) \\ \dot{y} &= x(\rho - z) - y \\ \dot{z} &= xy - \beta z \end{aligned} \quad (10)$$

With the following values in their coefficients.

$$\begin{aligned} \sigma &= 10 \\ \beta &= 8/3 \\ \rho &= 28 \end{aligned} \quad (11)$$

According to eq. (10) the positions $X = x, y, z$ are the independent variables with which we will generate Θ(X) and the accelerations $\dot{X} = \dot{x}, \dot{y}, \dot{z}$ are the dependent variables that we will describe from SINDy.

After simulating, generating the polynomial combinatorial search space and solving for Ξ, we obtain the structure and coefficients identified by SINDy as shown in eq. (12)

$$\Xi = \begin{bmatrix} 0 & 0 & 0 \\ -9.99999975 & 28.00000994 & 0 \\ 10.00000388 & -1.0000246 & 0 \\ 0 & 0 & -2.6666683 \\ 0 & 0 & 0 \\ 0 & 0 & 0.99999986 \\ 0 & -1.0000002 & 0 \\ 0 & 0 & 0 \\ \vdots & \vdots & \vdots \\ 0 & 0 & 0 \end{bmatrix}. \quad (12)$$

The first row of the Ξcorresponds to the coefficients identified for each dependent variable corresponding to the function of the first column of the search space matrix Θ, for the case of a polynomial combinatorial search space defined in eq. (4) the first value corresponds to unity, and for this identification all the coefficients present a value of zero. For the second row of the matrix Ξ following the order of the polynomial combinatorial search space we have that correspond to the coefficients assigned to the function x, for the dependent variables $\dot{x}, \dot{y}$. To finish with the example, in the fourth row the coefficients assigned to z, in the sixth to xy, and in the seventh to xz. From row 7 onwards of eq.(12) the matrix Ξ presents 0 in all its values. The rows of matrix Ξ follow the order of the columns of matrix Θ of the polynomial combinatorial combinatorial search space. So the mathematical model of the Lorenz attractor identified with SINDy is as follows.

$$\begin{aligned} \dot{x} &\approx 10(y - x), \\ \dot{y} &\approx x(28 - z) - y, \\ \dot{z} &\approx xy - \frac{8}{3}z. \end{aligned} \quad (13)$$

5. Identification of the equivalent unbalance

The model is dimensioned in the original work of Bonello (2002), in which several cases of dimensioned unbalance were tested at a constant RPM of 3100. For this study we worked with the dimensioned equivalent unbalance. Table 1 is an extract of the cases from the work of Bonello (2002) where the second column corresponds to the dimensionless values of the unbalance and the third to the dimensionalized values. The algebraic relation is shown in eq.(14)

$$\widehat{U} = \frac{u}{c_r}$$

$$U_{eq} = m_{eq}\, u \quad (14)$$

Where $\widehat{U}$ is the dimensionless unbalance, u is the eccentricity of the system, c_r is the viscosity of the oil film, m_{eq} is the effective weight in the "*journal*" (supported section of the shaft) and U_eq is the dimensioned "*journal*" unbalance.

Cases	$\widehat{U}$	U_{eq} [kg*m]
base	0.90	0.0034
1	0.74	0.0028
2	1.06	0.0040
3	1.47	0.0055

Table 1 Equivalent unbalance values
(Bonello 2002)

This change in the equivalent unbalance generates changes in the accelerations of eq. (1). Which in turn modify the behavior of the orbits of the support displacements shown in figure (2).

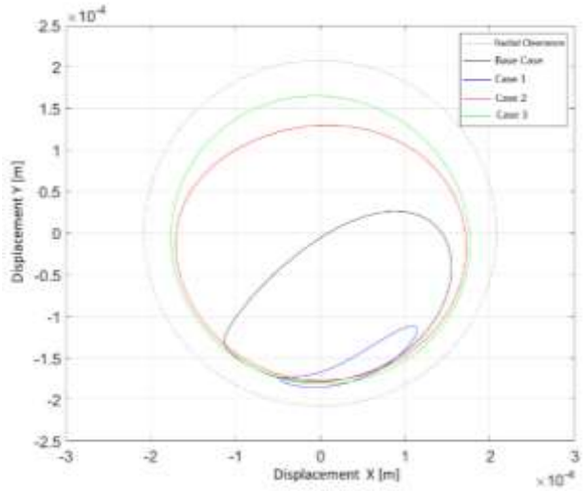

Figure 3 Behavior of the journal with different equivalent unbalances

From each of the simulations based on eq. (1) with the different cases mentioned, data were taken according to eq. (15) where X represents the set of independent variables and $\dot{X}$ the set of dependent variables with which SINDy will work. So it will identify 4 models in the form $\dot{X}(X)$.

$$\mathbf{X} = \left[\frac{Q_x}{M_{R,J}}, \frac{Q_y}{M_{R,J}}, \frac{\Omega^2 \sin \Omega t}{M_{R,J}}, \frac{\Omega^2 \cos \Omega t}{M_{R,J}}\right]$$

$$\dot{\mathbf{X}} = \left[\ddot{X}_J, \ddot{Y}_J\right] \quad (15)$$

The polynomial combinatorial search space will be generated with $K = 3$, so that $S = 35$, functions with which SINDy will perform the identification.

ISSN 2531-2979

On the first column of the search space, which represents the unit, a modification was made, multiplying it all by $W/M_{R,J}$,, to facilitate the process of identification of the imbalance by means of SINDy.

Exemplifying on the base case, taking into account the form of the search space of eq. (4) the matrix Ξ has the following structure;

$$\Xi = \begin{bmatrix} 0 & -1.00000541 \\ 1.00000126 & 0 \\ 0 & 1.00000479 \\ 0.00337285 & 0 \\ 0 & -0.00337282 \\ 0 & 0 \\ \vdots & \vdots \\ 0 & 0 \end{bmatrix}, \quad (16)$$

so that the coefficient of the first row corresponds to the function $W/M_{R,J}$ where it has a coefficient in the second row corresponding to the behavior of eq. (1) for $\ddot{Y}_J$. Continuing, the second row corresponds to the function $\frac{Q_x}{M_{R,J}}$ which has a coefficient in the first column corresponding to $\ddot{X}_J$. In such a way that by means of SINDy we identify the unbalance coefficient U_{eq} in X by analyzing the coefficient in row 4 in column 1 and for the unbalance in Y the coefficient in row 5 in column 2.

5.1 Introducción de Ruido al Sistema

In practice, it is common for the signals of the system vibration responses to be contaminated by noise. Therefore, in the present work noise is added to the signal of the vector $\ddot{\boldsymbol{X}}$, which are the accelerations of the "j*ournal*". Eq.(17) is employed to add noise,

$$SNR = 20\log_{10}\left(\frac{A_{señal}}{A_{ruido}}\right), \quad (17)$$

where $A_{señal}$ is the square root of the root mean squares (RMS) of the signal without noise and A_{ruido} is the RMS of the noise. The scenarios with noise that were analyzed in the present work are 20db, 25db and 30db.

6. Results

The identified coefficients with and without noise are the equivalent unbalance components in each Cartesian plane U_{eq,J_x} in U_{eq,J_y} are quite close to the actual coefficient present in the simulations. For the case of this study, the absolute value of the coefficients obtained by SINDy in the Y direction was reported.

		$U_{eq,SINDy}$ [kg*m]	
Cases	$U_{eq,real}$	U_{eq,J_x}	U_{eq,J_y}
base	0.0034	0.00337285	0.00337282
1	0.0028	0.00337285	0.0027404
2	0.0040	0.00396606	0.00397528
3	0.0055	0.00549583	0.0055019

Table 2 Equivalent Unbalances Identified in each case without noise

	$U_{eq,SINDy}$ [kg*m]	
Noise	U_{eq,J_x}	U_{eq,J_y}
db20	0.00337226	0.00337809
db25	0.00340334	0.00336725
db30	0.00340334	0.00336725

Table 3 Equivalent Unbalances Identified in the base case with noise

	$U_{eq,SINDy}$ [kg*m]	
Conditions	U_{eq,J_x}	U_{eq,J_y}
db20	0.00278523	0.00276609
db25	0.00275921	0.00278326
db30	0.00275921	0.00278326

Table 4 Equivalent Unbalances Identified in case 1 with noise

	$U_{eq,SINDy}$ [kg*m]	
Conditions	U_{eq,J_x}	U_{eq,J_y}
db20	0.0039892	0.00402207
db25	0.00398733	0.00398227
db30	0.00398733	0.00398227

Table 5 Equivalent Unbalances Identified in Case 2 with Noise

	$U_{eq,SINDy}$ [kg*m]	
Conditions	U_{eq,J_x}	U_{eq,J_y}
db20	0.00550924	0.00543415
db25	0.00548761	0.00548324
db30	0.00548761	0.00548324

Table 6 Equivalent Unbalances Identified in case 3 with noise

ISSN 2531-2979

The hyperparameters $K = 3$ and $\lambda = 0.001$ to identify the models remained static throughout the 4 cases under the different noise conditions.

6.1 Error

The error in each set of cases from table 2 to 6 is shown in table 7 to 11 following the same order as the cases presented. The error was calculated with eq. (18).

$$Error\ (\%) = \left|\frac{Valor_{real} - Valor_{SINDy}}{Valor_{real}}\right| \times 100 \qquad (18)$$

	Error (%) in	
Cases	U_{eq,J_x}	U_{eq,J_y}
base	0.7985	0.7994
1	1.1218	2.1286
2	0.8485	0.618
3	0.0758	0.0345

Table 7 Error of each Equivalent Unbalance Identified in the cases without noise.

	Error (%) in	
Noise	U_{eq,J_x}	U_{eq,J_y}
db20	0.8159	0.0644
db25	0.0982	0.9632
db30	0.0982	0.9632

Table 8 Error of each Equivalent Unbalance Identified in the base case

	Error (%) in	
Conditions	U_{eq,J_x}	U_{eq,J_y}
db20	0.5275	1.2111
db25	1.4568	0.5979
db30	1.4568	0.5979

Table 9 Error of each Equivalent Unbalance Identified in case 1

	Error (%) in	
Conditions	U_{eq,J_x}	U_{eq,J_y}
db20	0.27	0.5517
db25	0.3168	0.4432
db30	0.3168	0.4432

Table 10 Error of each Equivalent Unbalance Identified in case 2

	Error (%) in	
Conditions	U_{eq,J_x}	U_{eq,J_y}
db20	0.168	1.1973
db25	0.2253	0.3407
db30	0.2253	0.3407

Table 11 Error of each Equivalent Unbalance Identified in case 3

Observing the error of each case with and without noise, the coefficients are quite close to the real behavior.

7. Analysis of Results

Once the coefficients were identified in section 6, the vibrational response of the acceleration of the *"journal"* is simulated again in their respective Cartesian coordinates $\ddot{X}_J, \ddot{Y}_J$. Figures (3-6) show the comparison of the reference response and the different noise scenarios in which they were identified with the acceleration coefficients. With the figures it is corroborated that the error obtained in the system is minimal, having a very similar behavior between them. In figure (3) the black line corresponds to the real case, the segmented green line to the coefficients obtained by SINDy without noise, the magenta line to SINDy at 20db, the blue line to SINDy at 25db and finally the red line to SINDy at 30db. In each of the figures (3-6) there are two graphs, the upper graph corresponds to the acceleration in X and the lower one to the acceleration in Y, for both graphs the abscissa axis is the time of the last 20 cycles of the simulation.

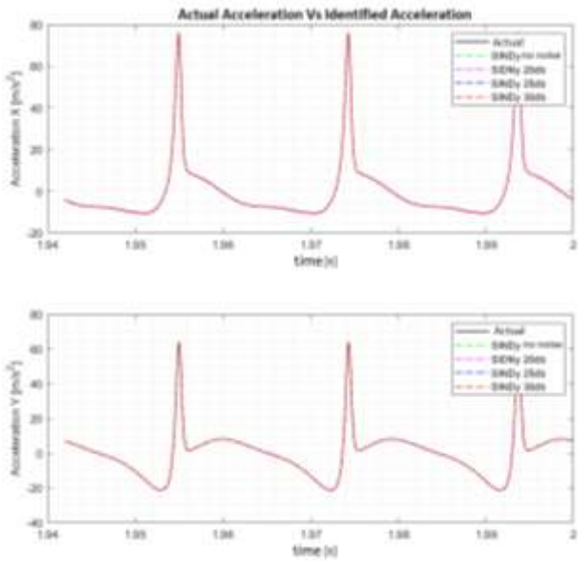

Figure 4 Actual Acceleration Vs Identified base case with and without noise

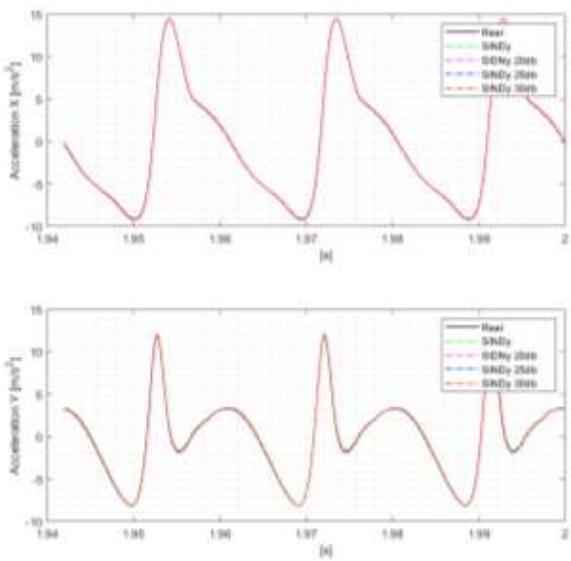

Figure 5 Actual Acceleration Vs Identified case 1 with and without noise

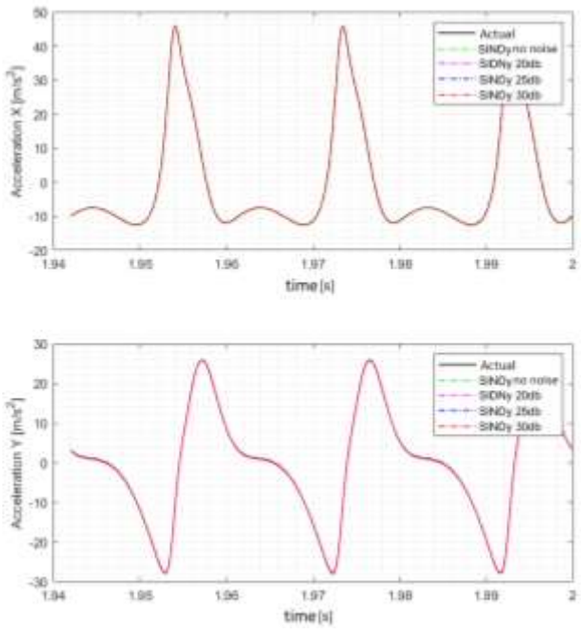

Figure 6 Actual Acceleration Vs Identified case 2 with and without noise

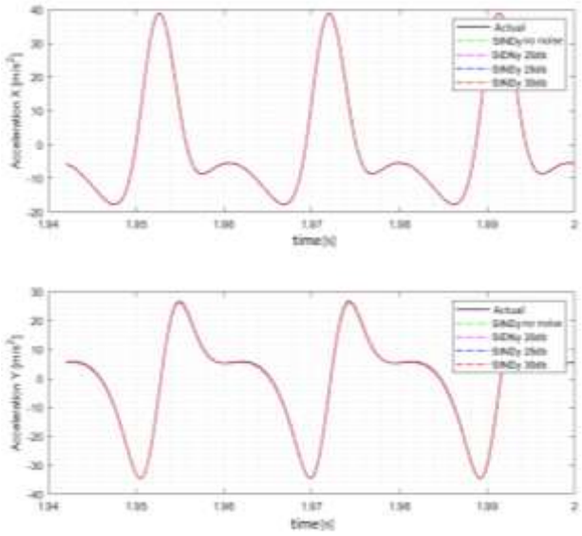

Figure 7 Actual Acceleration Vs Identified case 3 with and without noise

Similarly, with the obtained coefficients we simulate again to obtain the displacement orbits of each case, under the different noise conditions. In such a way that figures (7-10) are the different cases, where the dotted line is the radial clear, the black one the real case, the yellow one corresponds to the case without noise, the blue one to the case with noise of 20db, the red one to 25db and the green one to 30db. The axes of the figures correspond to the displacements.

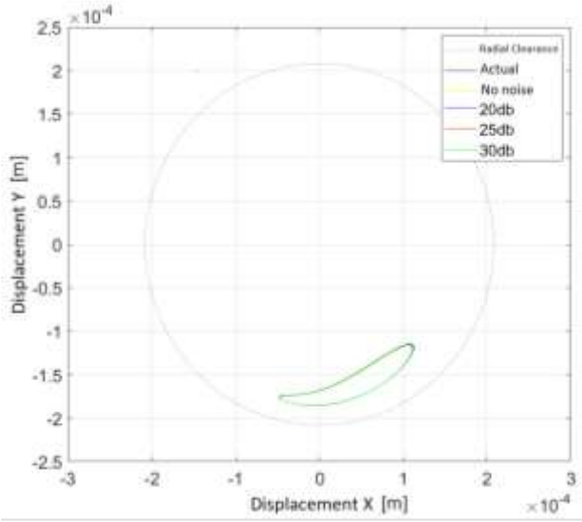

Figure 8 Actual displacement Vs Identified base case with and without noise

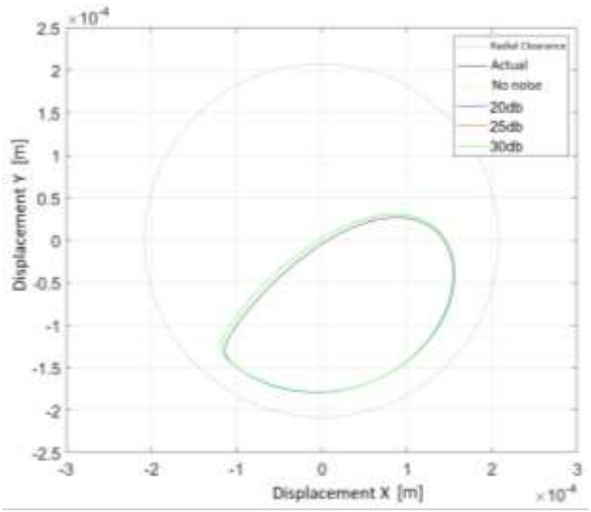

Figure 9 Actual displacement Vs Identified case 1 with and without noise

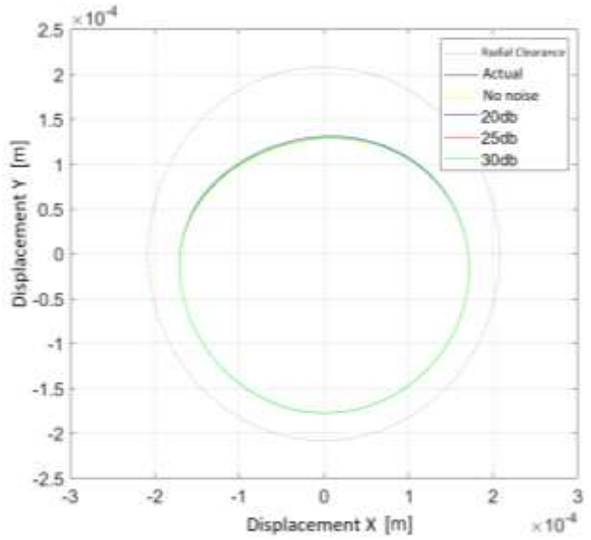

Figure 10 Actual displacement Vs Identified case 2 with and without noise

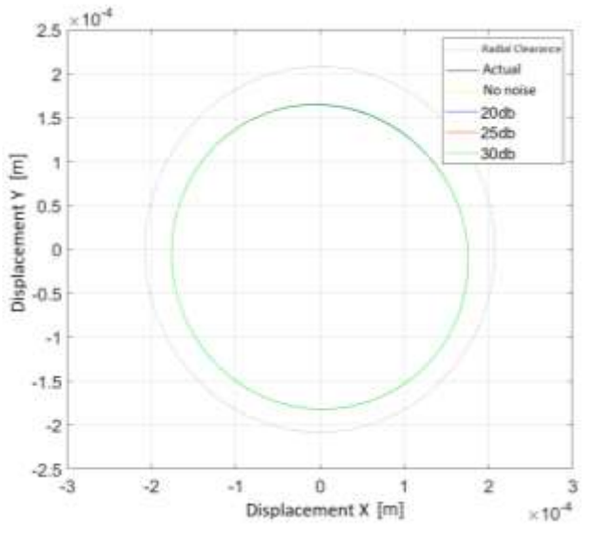

Figure 11 Actual displacement Vs Identified case 3 with and without noise

The base case at different noise magnitudes was the one that departs the most from the real behavior, however, this is not significant in the general behavior of the displacement. For cases 1, 2 and 3 at different noise conditions, it is observed that the displacement is practically identical to the real one.

8. Conclusions

An approach of autonomous learning methodologies was applied to solve an aeronautical problem. The SINDy algorithm was applied employing a polynomial combinatorial search space. The study was successfully performed to identify the equivalent imbalance in a SFD type support. Four cases of different equivalent imbalances were identified at 4 different noise conditions. The percentage of error presented in the identified coefficients is negligible, this is verified through the figures (3-10), where it can be observed that the behavior of the displacements and accelerations between the real case and those identified with SINDy do not present significant differences neither quantitatively nor qualitatively.

This work is an approach to solve engineering problems through *machine learning* methods, and it is an excellent first approach to use SINDy in rotodynamics problems. These methodologies are promising for solving more complex problems in the area of rotodynamics. We plan to use SINDy to solve inverse problems as future work.

Acknowledgments

We thank the UNAM-PAPIIT projects IN113921 and IN118820 for the computational resources used for this article. We also thank the IPN-SIP 20220976 project for the support to present the results obtained in this congress. We would also like to thank CONACYT for their support through the national scholarship program and the researcher system (SNI).

References

Bonello P. (2002). The non-linear modelling of squeeze film damped rotor-dynamic systems: an efficient integrated approach. [Tesis doctoral, University of Southampton].

ISSN 2531-2979

Brunton, Steven L., Proctor Joshua L. & Kutz J. Nathan (2016, 28 de marzo). Discovering governing equations from data by sparse identification of nonlinear dynamical systems. Proceedings of the National Academy of Sciences, 113(15), 3932-3937. https://doi.org/10.1073/pnas.1517384113

Brunton, Steven L., Noack, Bernd R. & Koumoutsakos, Petros (2020, 1 de mayo). Machine Learning for Fluid Mechanics. Annual Review of Fluid Mechanics, 52(1), 477-508. https://doi.org/10.1146/annurev-fluid-010719-060214

Dicken V., P. Maaß, I. Menz , J. Niebsch & R. Ramlau (2007, 26 de enero). Nonlinear inverse unbalance reconstruction in rotor dynamics. Inverse Problems in Science and Engineering, 13(5), 507-543. https://doi.org/10.1080/17415970500104234

Holmes, R., & Dogan, M. (1982). Investigation of a Rotor Bearing Assembly Incorporating a Squeeze-Film Damper Bearing. Journal of Mechanical Engineering Science, 24(3), 129–137. https://doi.org/10.1243/JMES_JOUR_1982_024_026_02

San Andres L. (2018, 11 de mayo). Squeeze Film Dampers Do's and Don'ts. [Presentación de Conferencia]

Torres Cedillo S. G., Ghaith Ghanim Al-Ghazal, Bonello P., Cortés Pérez J., (2019). Improved non-invasive inverse problem method for the balancing of nonlinear squeeze-film damped rotordynamic systems. Mechanical Systems and Signal Processing. 117, 569-593. https://doi.org/10.1016/j.ymssp.2018.07.032

.

ISSN 2531-2979